

Aperture optical antennas

Jérôme Wenger

CNRS, Aix-Marseille Université, Centrale Marseille, Institut Fresnel, UMR 7249, 13013 Marseille, France

Corresponding author: jerome.wenger@fresnel.fr

1 Introduction

Light passing in a small aperture is the subject of intense scientific interest since the very first introduction of the concept of *diffraction* by Grimaldi in 1665 [1]. This interest is directly sustained by two facts: an aperture in an opaque screen is probably the simplest optical element, and its interaction with electromagnetic radiation leads to a wide range of physical phenomena. As the fundamental comprehension of electromagnetism as well as the fabrication techniques evolved during the twentieth century, the interest turned towards apertures of subwavelength dimensions. Bethe gave the first theory of diffraction by an idealized subwavelength aperture in a thin perfect metal layer [2], predicting extremely small transmitted powers as the aperture diameter decreased far below the radiation wavelength. These predictions were refuted by the observation of the so-called extraordinary optical transmission phenomenon by Ebbesen and coworkers in 1998 [3], which in turn stimulated much fundamental research and technology development around subwavelength apertures and nano-optics over the last decade [4–6]. It is not the aim of this chapter to review the transmission of light through subwavelength apertures. Comprehensive reviews can be found in [7] and [8]. Instead, this chapter will focus on subwavelength apertures to reversibly convert freely propagating optical radiation into localized energy, and tailor light-matter interaction at the nanoscale. This goes within the rapidly growing field of optical antennas [9, 10], which forms the core of this book.

From a general perspective as discussed in antennas textbooks [11, 12], antennas can be classified into four basic types: electrically small antennas (of very short dimensions relative to the wavelength), resonant antennas (which include common designs such as dipole, patch and Yagi-Uda antennas), broadband antennas (which operate over an wide frequency range, such as spiral or log-periodic antennas), and lastly aperture antennas. Apertures thus define a type of antennas on their own, the aperture opening determining an obvious effective surface for collecting and emitting waves. The microphone, the pupil of the human eye and the parabolic reflector for satellite broadcast reception can all be considered as examples of aperture antennas. Electromagnetic aperture antennas operate generally at microwave frequencies, and are most common for space and aircraft applications, where they can be conveniently integrated into the spacecraft or aircraft surface without affecting its aerodynamic profile.

The aim of this chapter is to review the studies on subwavelength aperture antennas in the optical regime, paying attention to both the fundamental investigations and the applications. Section 2 reports on the enhancement of light-matter interaction using three main types of aperture antennas: single subwavelength aperture, single aperture surrounded by shallow surface corrugations, and subwavelength aperture arrays. A large fraction of nanoaperture applications is devoted to the field of biophotonics to improve molecular sensing, which are reviewed in Section 3. Lastly, the applications towards nano-optics (sources, detectors and filters) are discussed in Section 4.

2 Enhanced light-matter interaction on nanoaperture antennas

2.1 Single apertures

The introduction of the concept of subwavelength aperture antennas to improve optical systems can be attributed to E. H. Synge for his pioneering vision of scanning near field microscopy [13]. However, the first practical use of subwavelength apertures to enhance light-matter interaction dates back to 1986 [14]. In this study, apertures of diameters down to 180 nm fabricated in silver or gold films on glass slides were used as substrates to detect fluorescent molecules, and clear indications of fluorescence enhancement were reported. Fluorescence enhancement for single molecules in a single subwavelength aperture was reconsidered in 2005, and a 6.5 fold enhancement of the fluorescence rate per rhodamine 6G molecule was reported while using a single 150 nm diameter aperture milled in an opaque aluminum film [15]. This result, and the broad interest devoted to the phenomenon of extraordinary optical transmission [7], led to a large number of studies to understand the physical origins of the phenomenon, investigate the role of several design parameters (aperture shape and dimensions, metal permittivity, metal adhesion layer), and develop practical applications (Figure 1).

Influence of the metal layer and aperture diameter was thoroughly investigated in reference [16]. Comparison with numerical simulations reveals that the fluorescence enhancement is maximum when the aperture diameter corresponds to a minimum of the group velocity of light inside the hole [17]. This provides a guideline for the design of optimized nanostructures for enhanced fluorescence detection. For applications in the UV part of the spectrum, aluminum apertures provide the highest enhancement factors, with a 20x net increase in tryptophan molecules fluorescence for 75 nm diameter apertures in aluminum [18]. For applications in the near-infrared, gold is the metal of choice, if sufficient care is taken to properly design the adhesion layer used between the gold film and glass substrate. Any increase in the absorption losses due to the adhesion layer permittivity or thickness was demonstrated to lower the fluorescence enhancement in subwavelength apertures [19], and more generally plasmonic antennas. This effect was related to a damping of the energy coupling at the nanoaperture while using absorbant adhesion layers such as chromium or titanium. Optimisation of the various design parameters (200 nm thick gold layer, 10 nm titanium dioxide adhesion layer, 120 nm circular aperture diameter) led to the largest fluorescence enhancement factor found for single apertures (25x for Alexa Fluor 647 molecules of 30% quantum yield in water solution) [19]. Selecting a molecule with lower quantum yield would further increase the apparent fluorescence enhancement factor, with an upper limit of 50x enhancement for quantum emitters with quantum yield below 1% [20]. Higher enhancement factors could be in principle achieved with silver films thanks to lower ohmic losses in silver as compared to gold. However, the chemical reactivity of silver makes challenging any experiment with organic fluorophores.

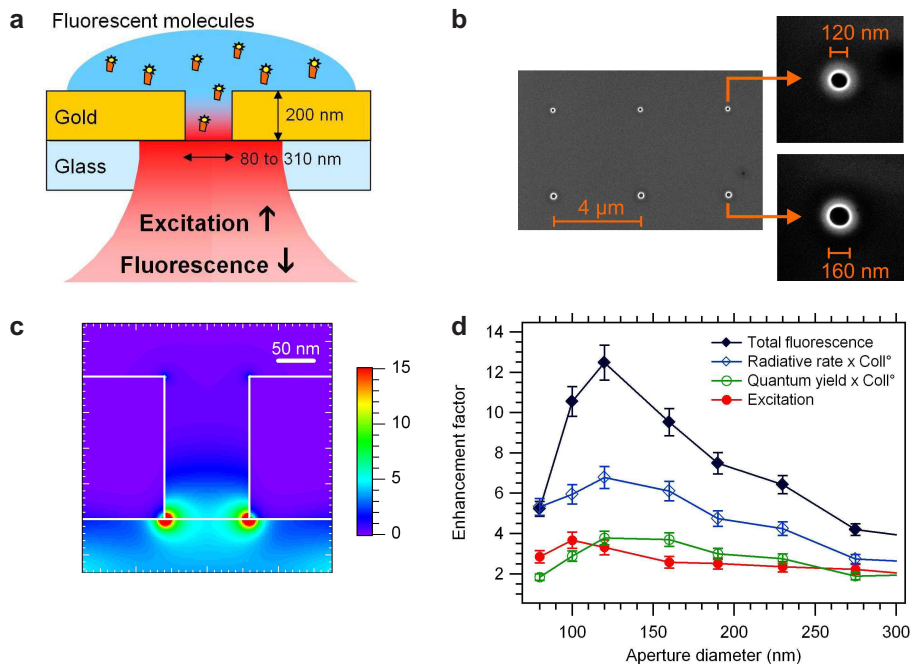


Figure 1: (a) Single subwavelength aperture to enhance the fluorescence emission of molecules located inside the structure [21]. (b) Electron microscope images of 120 and 160 nm apertures milled in gold. (c) Field intensity distribution on a 120 nm water-filled gold aperture illuminated at 633 nm [23]. (d) Fluorescence enhancement factor and contributions to nanoaperture enhanced fluorescence of emission and excitation enhancement, plotted versus the aperture diameter and normalized to the open solution case, from [21]. Figures reproduced with permission: (a,d) © OSA 2008, (b,c) © ACS 2010.

The physical phenomena leading to the fluorescence enhancement in single subwavelength apertures were investigated in reference [21]. By combining methods of fluorescence correlation spectroscopy and fluorescence lifetime measurements, the respective contributions of excitation and emission were quantified (Figure 1d). Excitation and emission enhancement mechanisms were also investigated numerically [22], including a spectral study for individual gold apertures. Fluorescence quenching was clearly observed for aperture diameters much below the cut-off diameter of the fundamental mode that may propagate through the aperture. This explains the existence of an optimum diameter for maximum enhancement. Lastly, the excitation intensity enhancement was further confirmed by an independent study monitoring the transient emission dynamics of colloidal quantum dots in subwavelength apertures [23].

Apart from fluorescence, subwavelength apertures were also demonstrated to enhance a broad range of different light-matter interactions. Second harmonic generation (SHG) was first investigated for large (> 500 nm) apertures [24], then for subwavelength apertures (circular and triangular) with sizes down to 125 nm [25]. The SHG enhancement originates from a combination of field enhancements at the nanoaperture edge together with phase retardation effects. Triangular nanoapertures exhibit superior SHG enhancement compared to circular ones, as expected from their noncentrosymmetric

shape. Surface enhanced Raman scattering (SERS) was also characterized for single nanoapertures in gold using a non-resonant analyte molecule [26]. Thanks to their insensitivity to quenching losses, SERS and SHG provide essential complementary information to fluorescence-based studies, specially to quantify the excitation intensity enhancement at the aperture edge. For instance, a peak SERS enhancement factor of 2×10^5 was quantified for a 100 nm diameter aperture, corresponding to a peak intensity enhancement $|E_{\max}|^2 / |E_0|^2 > 200$ at the aperture edge (for the direction along the incident polarization). The increase of the local excitation intensity within subwavelength apertures also leads to other locally enhanced light-matter interactions, such as erbium up-conversion luminescence [27], or biexciton state formation rate in semiconductor quantum dots [23].

The first studies on aperture-enhanced fluorescence were performed with circular holes, as this shape is polarization insensitive and relatively simple to fabricate with ion beam milling. Since 2005, several different aperture shapes have been considered. Slits [28,29], rectangles [30], and triangles [31] are polarization sensitive, providing an extra degree of freedom to tune the electromagnetic distribution inside the aperture, or polarize the emitted light. Coaxial apertures [32] or ring cavities [33] display narrower resonances and smaller mode volumes as compared to circular shapes, suggesting that high Purcell factors (> 2000) should be reached with such designs [33].

2.2 Single apertures surrounded by surface corrugations

Due to its subwavelength dimension, an isolated nanoaperture antenna does not provide a strong directional control on the light emitted from the aperture [16,34], although edge effects from the metallic walls have been reported in the case of single molecule fluorescence experiments [35]. From classical antenna theory [11,12], the IEEE directivity D of an aperture antenna can be expressed as $D = 4\pi(\text{area})/\lambda^2$, where *area* is the effective aperture area and λ is the radiation wavelength. Thus for a circular aperture of diameter d , the directivity is $D = (\pi d/\lambda)^2$, which shows that the directivity vanishes for a subwavelength aperture ($d \ll \lambda$).

Adding concentric surface corrugations (or grooves) on the metal around the central aperture is an elegant way to increase the effective aperture area while keeping the subwavelength dimensions of the aperture [36] (Figure 2a). This antenna design merges the light localization from the nanoaperture with the extended near to far-field conversion capabilities from the concentric grooves. When the corrugations are milled on the input surface ('reception' mode), the grating formed by the corrugations provide the supplementary momentum required to match the incoming light to surface plasmon modes, which further increase the light intensity at the central aperture. When the corrugations are milled on the output surface ('emission' mode), the reverse phenomenon appears, the surface corrugations couple the surface waves back to radiated light into the far-field. As the coupling of far-field radiation into surface plasmon modes is governed by geometrical momentum selection rules, the coupling occurs preferentially at certain angles for certain wavelengths. These principles were originally demonstrated in pioneering transmission experiments on corrugated apertures [36], and confirmed by surface second harmonic generation experiments [37].

Corrugated aperture antennas appear thus as an excellent design to fully control the radiation from single quantum emitters, providing high local intensity enhancement together with emission directionality. Moreover, this design is suitable for the detection of emitters in liquid solution diffusing inside the central aperture, thanks to strong localization of light inside the aperture. Two independent studies have recently demonstrated these principles for organic fluorescent molecules [38,39] and

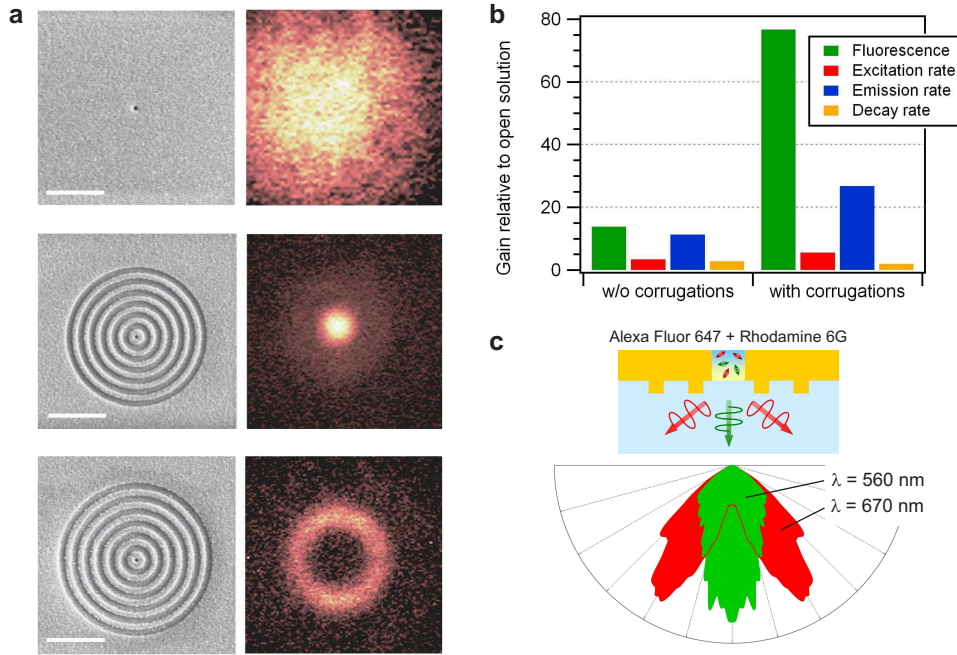


Figure 2: (a) Scanning electron microscope images of corrugated apertures (scale bar $2 \mu\text{m}$) and scanning confocal images of quantum dot photoluminescence taken in a plane $10 \mu\text{m}$ below the aperture surface (scan size $15 \mu\text{m}$). From top to bottom: single 120 nm aperture, antenna with concentric grooves of 350 nm period, and antenna with a larger groove period of 420 nm [40]. (b) Fluorescence enhancement factor and contributions of excitation and emission gains, in the case of a single aperture with five corrugations [38]. Decay rate corresponds to the reduction of the fluorescence lifetime. (c) Fluorescence radiation pattern at two different emission wavelengths illustrating the directional photon sorting capability of corrugated apertures, from [39]. Figures reproduced with permission: (a) © NPG 2011, (b,c) © ACS 2011.

colloidal quantum dots [40]. Fluorescence enhancement factors up to 120 fold simultaneous with narrow radiation pattern into a cone of $\pm 15^\circ$ have been reported using a nanoaperture surrounded by 5 circular grooves [38] (Figure 2b). The fluorescence beaming results from an interference phenomenon between the fluorescence emitted directly from the central aperture and the surface-coupled fluorescence scattered by the corrugations [39,40]. Tuning the corrugations period or the distance from first corrugation to central aperture enables a wide control over the fluorescence directionality, in very close fashion to enhanced transmission experiments [41,42] (Figure 2a and c). In this framework, the exhaustive investigation of the design parameter space for enhanced transmission through corrugated apertures [43] is of major importance to further optimize the performances of corrugated aperture antennas. For fluorescence emission, the influence of the number of corrugations has been quantitatively investigated in [44], showing that a single concentric groove already provides a supplementary 3.5-fold increase in the fluorescence enhancement as compared to a bare nanoaperture, as suggested theoretically in [45]. The ability of surface corrugations to provide for large intensity and radiation

directionality has also stimulated several other studies to locally enhance Raman scattering [46] and four wave mixing [47], and to improve the performance of dipolar-like optical nanoantennas [48, 49].

2.3 Aperture arrays

Arranging the apertures in an array with periodic lattice is another way to provide for the momentum needed to match the far-field radiation with surface electromagnetic waves (Figure 3a). These extra coupling capabilities have largely stimulated several studies on extraordinary optical transmission for aperture arrays [3, 7]. Broadly speaking, two types of resonant phenomenon contribute to explain the transmission peaks observed in far-field and the intensity enhancement in the near field. The first phenomenon relies on the resonant excitation of surface plasmon waves at the metal-dielectric interface, which is obtained at specific incident angles and wavelengths according to grating diffraction rule. The second contribution comes from localized plasmon modes on properly shaped apertures. Combination of these two resonant phenomena are of major interest to locally enhance light-matter interaction, and control the radiation spectrum, direction and polarization.

Fluorescence enhancement for emitters dispatched over a subwavelength aperture array was first reported in [50–53] for organic molecules, then in [54] for colloidal quantum dots. Under resonant transmission conditions, the fluorescence enhancement normalized to the aperture array area was estimated to nearly 40 [50], while disordered ensemble of apertures lacking spatial coherence displayed much lower enhancement factors of about 7 [52] (Figure 3b). Maximum fluorescence signal is found under conditions of enhanced transmission of the excitation light and excitation of surface plasmons. Resonant coupling conditions are achieved either by selecting the incidence angle [50, 52], or by adjusting the array lattice [53–55]. Most experiments are performed in transmission mode, yet reflection mode also displays fluorescence enhancement and beaming [56].

Tuning the aperture shape provides further control on the local intensity enhancement inside the aperture, as the local resonances inside the aperture are independent on the incident angle. Enhancement of erbium ions photoluminescence and up-conversion luminescence was demonstrated for arrays of annular apertures, which exhibit a strong transmission resonance [57, 58] (Figure 3c). Changing the aperture shape also influences the amount of second harmonic generated by the metallic aperture arrays [59, 60]. For rectangular apertures the maximum second harmonic enhancement is obtained for the shape corresponding to the cutoff (or equivalently slow propagation) of the fundamental wavelength through the apertures [60] (Figure 3d). A similar effect was observed for fluorescence on single apertures [16, 30].

3 Biophotonic applications of nanoaperture antennas

3.1 Enhanced fluorescence detection and analysis

The confinement of light within a single subwavelength aperture and the local electromagnetic intensity increase are of major interest to develop new methods for fluorescence analysis down to the single emitter level. This subsection describes the different approaches along that direction.

Single molecule fluorescence spectroscopy in liquids The smallest volumes that can be achieved by diffraction-limited confocal microscopy are about a fraction of femtoliter ($1 \text{ fL} = 1 \mu\text{m}^3$). To ensure

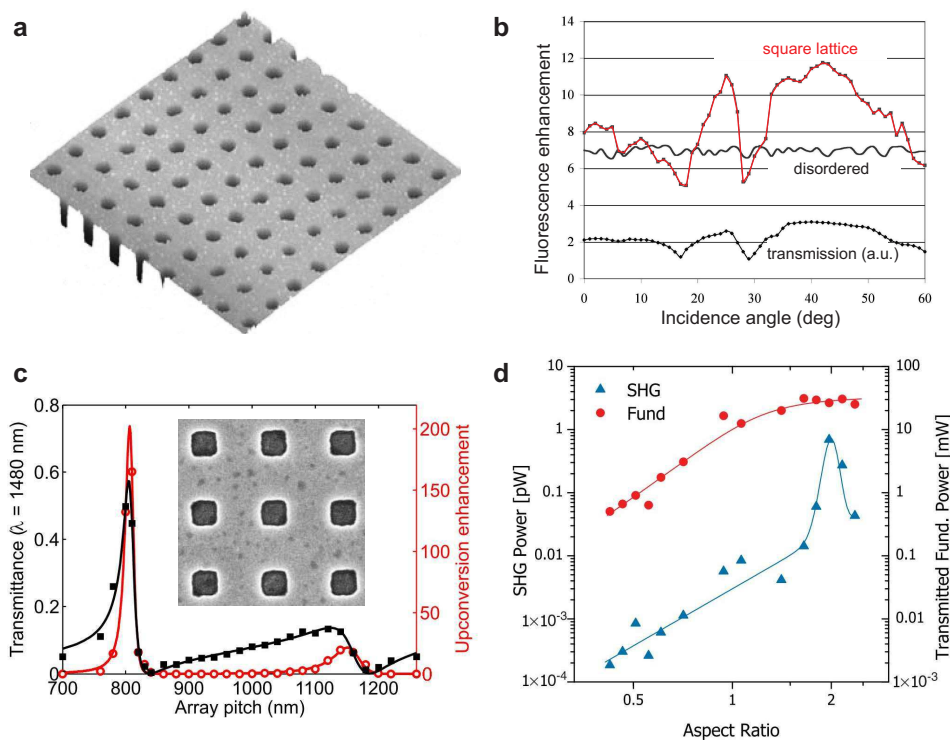


Figure 3: (a) AFM images of 200 nm diameter aperture array with 1 μm period [104]. (b) Fluorescence enhancement from Cyanine-5 from a periodic arrangement of 200 nm diameter apertures in 70 nm thick gold film, with 1 μm spacing. Fluorescence from a disordered array and transmission of the excitation light are also plotted for reference. Enhancement factors are normalized to a quartz slide with the same molecular monolayer, and corrected for fill fraction, adapted from [104]. (c) Comparison between the 980 nm erbium up-conversion enhancement (red) and the transmittance at 1480 nm (black) as a function of the array period [58]. (d) Second harmonic generated power (triangles) and fundamental light transmission (circles) as a function of aperture aspect ratio [60]. Figures reproduced with permission: (a,b) © IOP 2004, (c) © OSA 2009, (d) © APS 2006.

that only one molecule is present in such volumes, the concentration has to be lower than 10 nanomolar. Unfortunately, this concentration is too low to ensure relevant reaction kinetics and biochemical stability, which typically require concentrations in the μM to the mM range [61–63]. There is thus a very large demand for nanophotonic structures to overcome the limits set by diffraction, in order to (i) enhance the fluorescence brightness per emitter, and (ii) increase the range of available concentrations by reducing the observation volume. Several photonic methods have been developed during the last decade, as reviewed in [64]. Among them, subwavelength apertures bear the appealing properties of providing the smallest volumes and the highest fluorescence enhancement to date.

The introduction of subwavelength apertures to reduce the analysis volume in single molecule fluorescence spectroscopy was performed by the groups of Harold Craighead and Watt Webb in an outstanding contribution [61]. A subwavelength aperture milled in an opaque metallic film is an

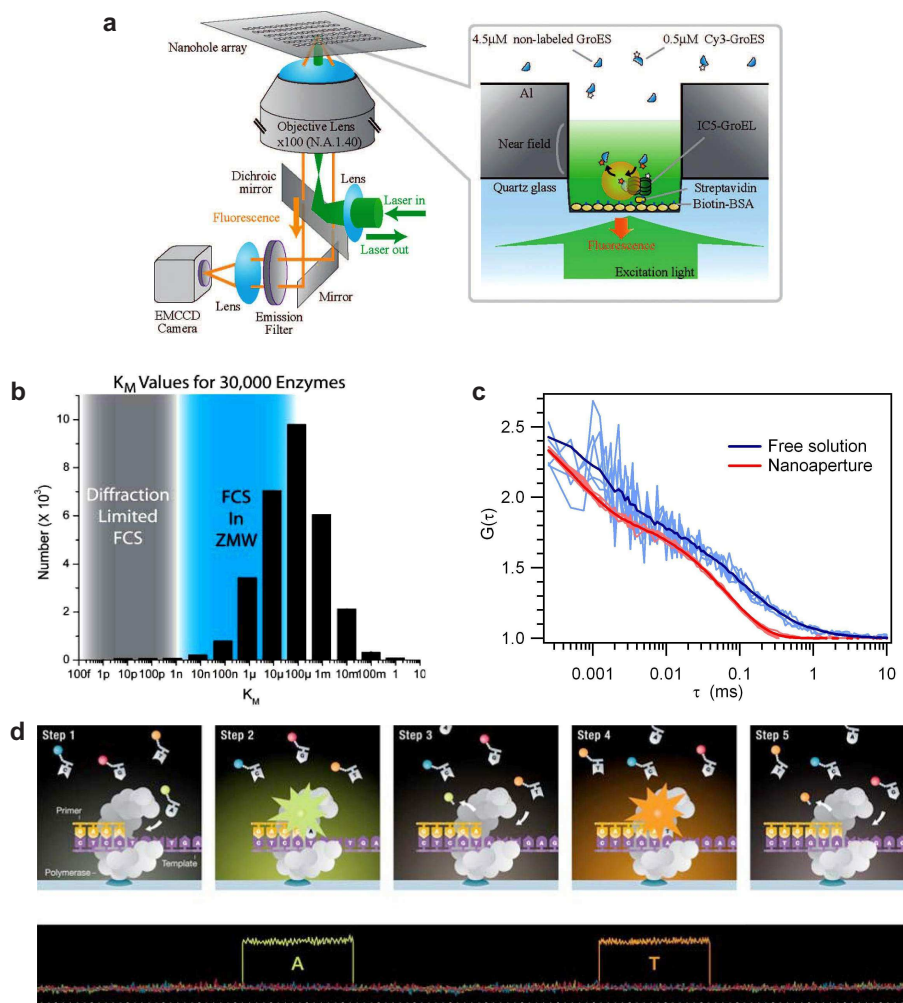


Figure 4: (a) Subwavelength aperture antennas for the detection and analysis of protein-protein interaction [67]. (b) Histogram of Michaelis constants for 30,000 enzymes, showing the range accessible to conventional diffraction-limited FCS and FCS with nanoapertures (ZMW) [62]. (c) Fluorescence correlation functions for 1 s integration time (thin lines). Thick lines correspond to averaging over 200 s [66]. Fast FCS measurements are enabled by the fluorescence enhancement in a nanoaperture. (d) Single-molecule real-time DNA sequencing performed while incorporation of individual nucleotides is followed, the lower trace displays the temporal evolution of the fluorescence intensity [68]. Figures reproduced with permission: (a) © ACS 2008, (b) © BS 2005, (c) © ACS 2009, (d) © Pacific Biosciences Inc.

elegant way to generate an analysis volume much below the diffraction limit (Figure 4a), enabling single molecule analysis at much higher concentrations (Figure 4b). Subwavelength apertures have thus been termed zero-mode waveguides or ZMW to emphasize the evanescent nature of the excitation light inside the aperture. A large range of biological processes have been monitored with single molecule resolution

at micromolar concentrations while using nanoapertures. This includes DNA polymerase activity [61], oligomerization of the bacteriophage λ -repressor protein [62], DNA enzymatic cleavage [65,66], and protein-protein interactions [67]. Moreover, the physical limitation of the observation volume by the nanoaperture greatly simplifies the optical alignment for multi-color cross-correlation analysis [65]. The high fluorescence count rates improve the signal to noise ratio by over an order of magnitude, enabling a 100-fold reduction of the experiment acquisition time [66] (Figure 4c). This offer new opportunities for probing specific biochemical reactions that require fast sampling rates.

DNA sequencing The development of personalized quantitative genomics requires novel methods of DNA sequencing that meet the key requirements of high-throughput, high-accuracy and low operating costs simultaneously. To meet this goal, subwavelength apertures are currently being used as nano-observation chambers for single-molecule, real-time DNA sequencing [68,69] (Figure 4d). Within each aperture, a single DNA polymerase enzyme is attached to the bottom surface [70], while distinguishable fluorescent labeled nucleotides diffuse into the reaction solution. The sequencing method records the temporal order of the enzymatic incorporation of the fluorescent nucleotides into a growing DNA strand replicate. Each nucleotide replication event last a few millisecond, and can be observed in real-time. Currently, over 3000 nanoaperture are operated simultaneously, allowing straightforward massive parallelization [68].

Live cell membrane investigations Investigating the cell membrane organization with nanometer resolution is a challenging task, as standard optical microscopy does not provide enough spatial resolution while electron microscopy lacks temporal dynamics and cannot be easily applied to live cells [71]. A subwavelength aperture provides a promising tool to improve the spatial resolution of optical microscopy. Contrarily to near-field scanning optical microscopy (NSOM), the subwavelength aperture probe is fixed to the substrate, with a cell being attached above (Figure 5a,b). The aperture works as a pinhole directly located under the cell to restrict the illumination area. Diffusion of fluorescent markers incorporated into the cell membrane provide the dynamic signal, which is analyzed by correlation spectroscopy to extract information about the membrane organization [72,73]. To gain more insight about the membrane organization, measurements can be performed with increasing aperture diameters [74–76] (Figure 5c). This set of experiments demonstrated the aperture limited the observed membrane area, and did not significantly alter the diffusion process within the membrane. It was also shown that fluorescent chimeric ganglioside proteins partition into structures of 30 nm radius inside the cell membrane [74]. The combinaison of nanoapertures with fluorescence correlation spectroscopy on membranes provide a method having both high spatial and temporal resolution together with a direct statistical analysis. The major limitation of this method is directly related to the need for cell membranes to adhere to the substrate. Cell membrane invagination within the aperture was shown to depend on the membrane lipidic composition [73] and on actin filaments [77]. To further ease cell adhesion, and avoid membrane invagination issues, planarized 50 nm diameter apertures have been recently introduced [78]. The planarization procedure fills the aperture with fused silica, to achieve no height distinction between the aperture and the surrounding metal. The technique provides 1 μ s and 60 nm resolution without requiring penetration of the membrane into the aperture.

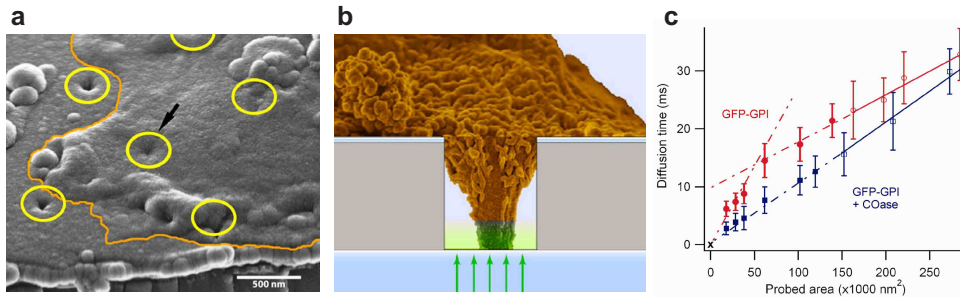


Figure 5: (a) Tilted scanning electron microscope view of cross-sectional cuts of nanoapertures. Cell membranes have been outlined (orange line), and aperture locations have been circled (yellow). Cell membrane spanning a nanoaperture dips down (arrow), suggesting membrane invagination [77]. (b) Cross-sectional cartoon of cell invaginating into a subwavelength aperture (not drawn to scale; the shape of the membranous extension into the aperture is hypothetical) [77]. (c) Molecular diffusion times versus aperture area for untreated GFP-GPI protein and GFP-GPI with 1 U/mL cholesterol oxidase (COase) to reveal for transient diffusion regimes related to membrane heterogeneities on the nanometer scale [74]. Figures reproduced with permission: (a,b) © IOP 2007, (c) © BS 2007.

Trapping Optical tweezers have become a powerful tool for manipulating nano to micrometer sized objects, with applications in both physical and life sciences. To overcome the limits set by the diffraction phenomenon in conventional optics and extend optical trapping to the nanometer scale, metallic nanoantennas have been recently introduced and reviewed in [79]. Most works on plasmon nano-optical tweezers rely on a strong enhancement of the local intensity provided by the nanoantenna. This approach induces high local intensities, often above the objects damage threshold. A subwavelength aperture can solve this challenge, and achieve more than an order of magnitude reduction in the local intensity required for optical trapping [80] (Figure 6). The optical trapping method is called self-induced back-action (SIBA), as the trapped object plays an active role in enhancing the restoring force. Trapping of a single 50 nm polystyrene sphere was demonstrated based on the transmission resonance of a 310 nm diameter aperture in a gold film [80]. Remarkably, the local intensity inside the aperture is only enhanced by a moderate factor of seven. Low-intensity optical trapping of nanoparticles enables new opportunities for isolating and studying biological nano-objects, such as viruses. This trapping method can also be coupled directly to sensing and sorting based on transmission changes through the aperture.

3.2 Molecular sensing and spectroscopy with aperture arrays

Sensors able to detect a specific type of molecules in real-time and with high sensitivity are a subject of intense research, and a major drive for the field of plasmonics. Compared to other nanoantenna arrays designed for plasmon-enhanced sensing, subwavelength apertures bear the specific advantages of presumably better robustness and higher reproducibility, as the fabrication is comparatively simpler and the mode of operation does not rely on ultra-high intensity enhancement. This subsection reviews the different spectroscopic applications of subwavelength aperture arrays.

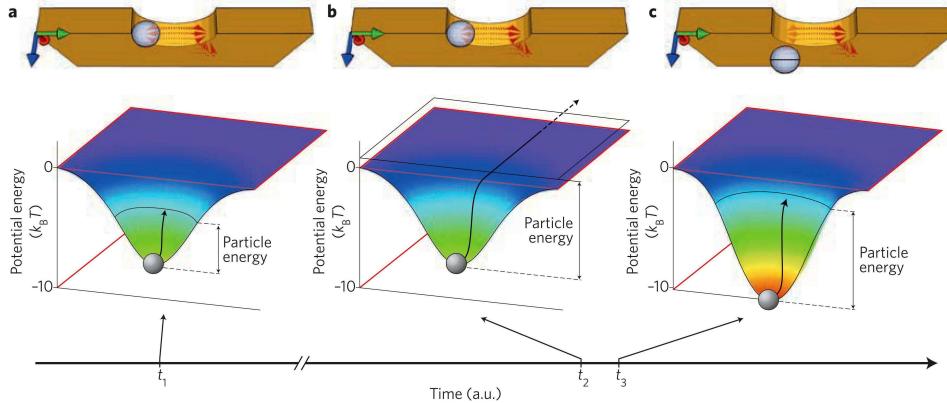


Figure 6: Self-induced back-action trapping, adapted from [79]. (a) The particle is localized in the aperture at time t_1 with moderate kinetic energy. (b) During a high-energy event at time t_2 , the object may escape the aperture. (c) As the particle moves out of the aperture at time t_3 , the SIBA force increases the potential depth to maintain the object within the trap. Figures reproduced with permission © NPG 2011.

Surface plasmon resonance spectroscopy Conventional surface plasmon resonance (SPR) sensing is based on the excitation of extended surface plasmon modes on a thin metal layer through prism coupling in the Kretschmann configuration. This method has proven to be sensitive to tiny refractive index changes at the metal surface down to the molecular monolayer level. The transmission of light through aperture arrays is also sensitive to refractive index changes around the metal [81] (Figure 7a). Currently, the sensitivity is comparable to other SPR devices, and molecular binding events can be followed dynamically by measuring a spectral shift in the transmitted light [82–84]. Nanoaperture arrays appear thus well suited for dense integration in a sensor chip in a collinear optical arrangement providing a simpler setup and a smaller probing area than the typical Kretschmann configuration. Current research directions include lan-on-chip integration with microfluidic systems [85–87], increasing the sensitivity [88, 89] and multiplexing the amount of extracted information [90, 91].

Isolated apertures or disordered patterns of apertures in thin gold films also exhibit a localized surface plasmon resonance leading to a peak in the extinction spectrum in the near-infrared region which can be used for sensing applications [92, 93]. This type of device has been successfully employed to monitor membrane biorecognition events [94, 95], and selective sensing for cancer antigens [96]. Aperture sensors can also be designed to work as nanopores, with the liquid flowing across the aperture arrays [97]. This configuration further improves the uptake rate of biomolecules and thus the sensing temporal resolution.

Enhanced absorption and fluorescence spectroscopy Nanoaperture arrays tuned for resonant transmission in the infrared were demonstrated to enhance the absorption of molecules adsorbed on the array by at least two orders of magnitude [98] (Figure 7b). Enhanced absorption spectroscopy can thus be used to monitor catalysis process [99] or phospholipid assembly [100]. The absorption enhancement is related to a long lifetime of surface plasmon modes in the infrared, which increases the interaction

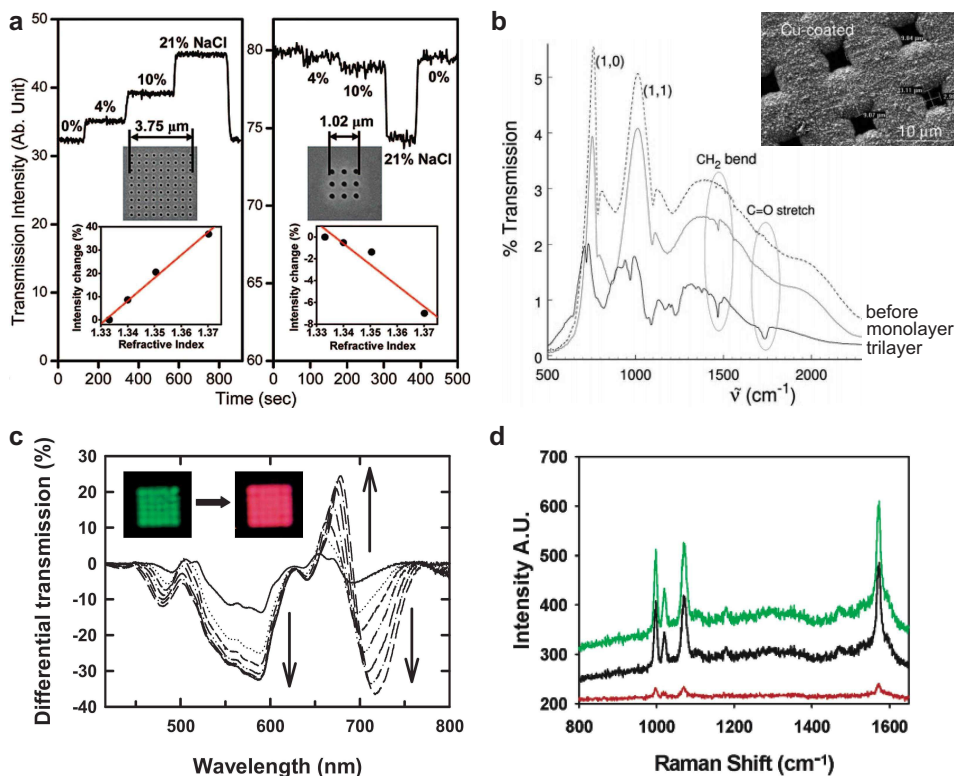


Figure 7: (a) Transmission response to surface refractive index change from a 9x9 and a 3x3 nanohole array [90]. (b) Infrared transmission spectra of copper-coated mesh before and after coating with 1-hexadecanethiol. There is significant damping of the transmission with the successive coatings, molecular absorptions are indicated with the solid ovals [100]. (c) Differential transmission of an array (period 390 nm, diameter 260 nm, depth 180 nm) covered with a spiropyran-doped PMMA film after different UV irradiation times (1 to 130 s). Arrows indicate the variation for increasing irradiation time. The insets show transmission images of the array before and after irradiation [101]. (d) Nanoaperture-enhanced Raman spectra of benzenethiol. The red spectrum was obtained from an unpatterned portion of the film; the black spectrum was obtained from a nanoaperture array with 450 nm lattice spacing. The green spectrum was corrected for the reduced geometric area on the array [113]. Figures reproduced with permission: (a) © ACS 2008, (b) © ACS 2006, (c) © Wiley-VCH 2006, (d) © ACS 2007.

probability between molecules and light. Absorption enhancement of electronic transitions was also reported in the visible [101], with lower enhancement factors of about one order of magnitude related to shorter plasmon lifetime or increased propagation losses (Figure 7c). Absorption enhancement is motivating new time-resolved spectroscopy studies to explore transient molecule-plasmon states [102, 103].

Enhancement of the fluorescence process was also used to perform DNA affinity sensing on aperture arrays spotted with probe DNA sequences [104]. Performing detection on the back-side of the aperture

sample provides high signal-to-background rejection, and enables real-time detection. Interestingly, capture of target molecules can be further improved by UV photoactivation of the aperture array silanized bottom surface [105]. This photoactivation procedure is a promising strategy to achieve localization of target molecules to the region of plasmonic enhancement.

Surface enhanced Raman spectroscopy Metallic nanostructures have attracted much interest over the last years to realize efficient and reproducible media for surface-enhanced Raman scattering (SERS) spectroscopy [106]. The major aim is to develop SERS substrates combining high sensitivity with control and localization of the regions leading to high SERS enhancement. Among the different strategies being explored, subwavelength apertures milled in noble metal films realize promising substrates thanks to their rational and tunable design, controlled surface enhancement, surfactant-free fabrication and intrinsic robustness (Figure 7d). The first SERS study with nanoaperture arrays was performed on resonant oxazine 720 dyes [107]. The enhancement factor reached a maximum for the array that presented the largest transmission at the excitation wavelength of the laser, which was confirmed by several other studies [108–112]. Reference [113] presents a remarkable quantitative study to determine the absolute Raman scattering enhancement factors for nanoaperture arrays in a silver film as a function of aperture lattice spacing, and using a nonresonant analyte. Maximum area-corrected SERS enhancement factor of 6×10^7 was obtained, which was attributed to two distinct sources: plasmons localized near the aperture edges and nanometer scale roughness associated with the silver film. Even higher enhancement factors could be reached by optimising further the aperture dimensions [26], or by performing SERS on more complex aperture antennas arrays, such as double-hole arrays [114] or combined aperture-nanoparticle pairs [115]. Lastly, the reproducibility of the SERS measurements was assessed in [116] for 2D hexagonal gold aperture arrays. Overall, area-averaged deviation from measurement to measurement ranged from 2 - 15%, which makes nanoaperture arrays a very competitive platform for sensitive and reproducible SERS.

4 Nanophotonic applications of nanoaperture antennas

4.1 Photodetectors and filters

Probably the most straightforward use of subwavelength aperture devices for photonic applications employs them as wavelength filters and polarisers. Periodic arrays display well-defined resonances depending on the lattice symmetry, period, aperture shape and lattice symmetry [3, 7, 8], and already an isolated rectangular aperture can be made as a wavelength and polarization sensitive filter [34]. Adding an elliptical plasmonic grating around a central subwavelength aperture realizes an antenna acting as a miniature planar wave plate [117]. The difference between the short and long axis of each ellipsis introduces a phase shift on the surface waves enabling the operation as a quarter wave plate.

A major bottleneck in the development of ultrafast photodetectors can be summarized as follows: to reduce the photodiode capacitance and increase its operational speed, the active semiconductor region needs to be reduced to sub-micron dimensions, yet this tiny active area also leads to low quantum efficiency and low sensitivity. The ability of shallow surface corrugations to concentrate light to the central aperture [36, 37] is highly beneficial to solve this challenge. Periodic corrugations on the metal surface act as resonant antennas to capture the incoming light, which can then be concentrated into one or more apertures filled with photovoltaic elements. Hence smaller photovoltaic elements can

still detect an enlarged amount of light energy. This principle was first demonstrated with 300 nm diameter silicon photodiode surrounded by a $10\ \mu\text{m}$ grating antenna [118] (Figure 8a), and was recently extended to telecom wavelengths with germanium photodiode [119]. Moreover, appropriate texturing of metal surfaces enables sorting the incoming light according to wavelength and polarization, before refocusing the energy into individual photodetector elements [120] (Figure 8b). This photon-sorting capability provides a new approach for spectral and polarimetric detectors with highly integrated architectures.

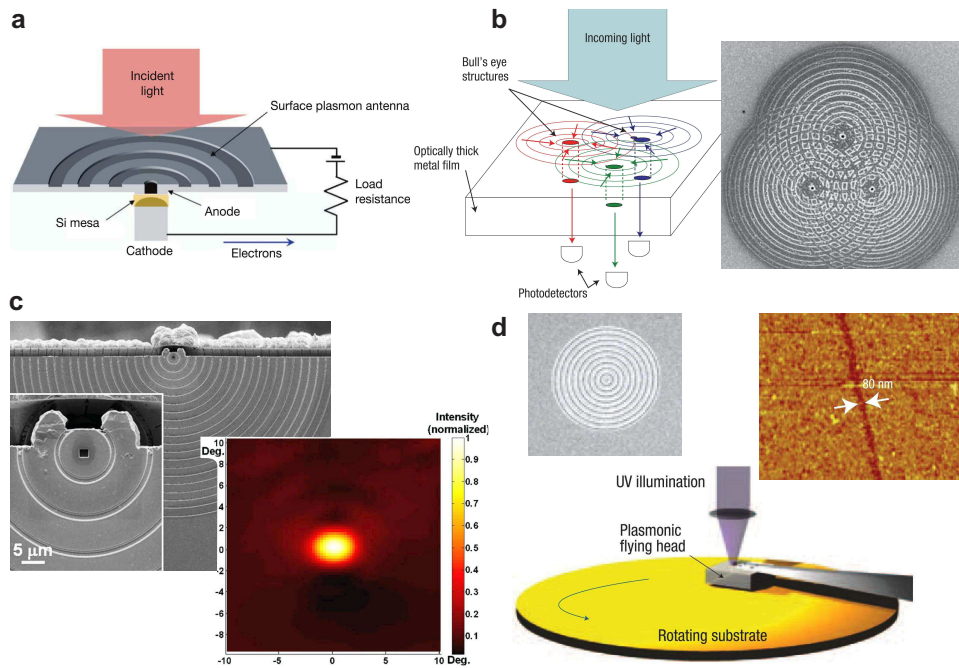


Figure 8: (a) Ultrafast nanophotodiode consisting of a 300 nm silicon photoelectric element integrated into a corrugated aperture antenna [118]. (b) Spatial filtering for the incoming white light through three overlapping corrugated aperture antennas. The different colours are separated as they couple to different gratings and are redirected towards three distinct photodetectors integrated inside the apertures. The inset shows an experimental realization with grating periods of 730 nm (top antenna), 630 nm (left), and 530 nm (right) [120]. (c) Quantum cascade laser integrated with a corrugated aperture collimator, and measured far-field intensity distribution [123]. (d) High-throughput maskless nanolithography using aperture antennas arrays, and AFM image of a pattern with 80 nm linewidth on the thermal photoresist [125]. Figures reproduced with permission: (a) © JJAP 2005, (b) © NPG 2008, (c) © AIP 2008, (d) © NPG 2008.

4.2 Nanosources

The antenna capabilities of corrugated apertures have attracted much attention to improve the performance of vertical-cavity surface-emitting lasers [121] and quantum cascade lasers emitting in the

infrared [122, 123]. Surface plasmons are used to shape the beams of edge or vertical surface emitting semiconductor lasers and greatly reduce their large intrinsic beam divergence (Figure 8c). Using concentric semi-circular grating structure, a collimated laser beam was achieved with remarkably small divergence angles of 2.7° and 3.7° , which correspond to a reduction by a factor of 30 and 10, compared to those without plasmonic collimation [123]. The grating antenna can also be modified to control the polarization of the laser beam, or achieve complex wavefront engineering [122]. As for lasers, the operation of light-emitting diodes (LEDs) can benefit from aperture antennas. Aperture arrays engraved in one of the electrodes provide an outcoupling mechanism for the trapped electromagnetic energy as well as a control over the emission properties [124].

The strong localization of electromagnetic energy with aperture antennas has stimulated a broad interest for achieving maskless subwavelength optical lithography, as an alternative to electron-beam and scanning-probe lithography (Figure 8d). Such direct lithography writing would be activated directly in the near field of the aperture, which makes it very difficult to scan the aperture above the surface at high speed. The first report introduced a self-spacing air bearing to fly the aperture about 20 nm above the photoresist with spinning speeds up to 12 m/s [125]. Recent advances have reported achievement of patterning with linewidth down to 50 nm and a patterning speed of 10 mm/s [126]. The same technique could also be applied to plasmonic-enhanced data storage, further improving the blu-ray disc capacity by about 2-fold [127].

5 Conclusion

Compared to nanoparticle-based plasmonic antennas, aperture antennas bear the essential advantage of providing a high contrast between the strong opacity of the metallic film and the aperture element. Although the local field enhancement are not as strong as in the case of bowtie antennas for instance [128–130], aperture antennas are comparatively simpler to fabricate and to implement, and readily provide for the high reproducibility needed in biosensing applications. Texturing the metal around the apertures opens novel opportunities to control the antenna operation. Further developments and applications are thus expected in the years to come in a variety of areas.

Acknowledgements

I am deeply indebted to many at the Fresnel Institute and the Laboratoire des Nanostructures at the Institut de Science et d'Ingénierie Supramoléculaires. I would like to gratefully acknowledge the collaboration with Hervé Rigneault and Thomas Ebbesen, together with my coworkers or collaborators: Heykel Aouani, Steve Blair, Nicolas Bonod, Eloïse Devaux, Davy Gérard, Pierre-François Lenne, Oussama Mahboub, Evgeny Popov, and Brian Stout.

References

- [1] Grimaldi, F.-M. in *Physico-mathesis de Lumine, Coloribus, et Iride*, Aliisque Sequenti Pagina Indicatis 9 (Bologna, 1665).
- [2] Bethe, H. A. "Theory of diffraction by small holes," *Phys. Rev.* 66, 163-182 (1944).

- [3] T. W. Ebbesen, H. J. Lezec, H. F. Ghaemi, et al., “Extraordinary optical transmission through subwavelength hole arrays,” *Nature* 391, 667-669 (1998).
- [4] W. L. Barnes, A. Dereux and T. W. Ebbesen, “Surface plasmon subwavelength optics,” *Nature* 424, 824-830 (2003).
- [5] L. Novotny and B. Hecht, “Principles of Nano-Optics,” (Cambridge University Press, Cambridge, 2006).
- [6] Schuller, J. A.; Barnard, E. S.; Cai, W. S.; Jun, Y. C.; White, J. S.; Brongersma, M. L. “Plasmonics for extreme light concentration and manipulation,” *Nature Mater.* 9, 193-204 (2010).
- [7] Garcia-Vidal, F. J.; Martin-Moreno, L.; Ebbesen, T. W.; Kuipers, L. “Light passing through subwavelength apertures,” *Rev. Mod. Phys.* 82, 729-787 (2010).
- [8] C. Genet, and T. W. Ebbesen, “Light in tiny holes,” *Nature* 445, 39-46 (2007).
- [9] Novotny, L.; van Hulst, N. “Antennas for light,” *Nature Photon.* 5, 83-90 (2011).
- [10] Bharadwaj, P.; Deutsch, B.; Novotny, L. “Optical Antennas,” *Adv. Opt. Photonics* 1, 438-483 (2009).
- [11] Balanis, C. A. “Antenna Theory Analysis and Design,” Third edition, John Wiley & Sons, Inc. (Hoboken, New Jersey, 2005).
- [12] Stutzman, W. L.; Thiele, G. A. “Antenna Theory and Design,” Second edition, John Wiley & Sons, Inc. (Hoboken, New Jersey, 1998).
- [13] E. H. Synge, “A suggested method for extending the microscopic resolution into the ultramicroscopic region,” *Philos. Mag.* 6, 356-362 (1928).
- [14] U. C. Fischer, “Submicrometer aperture in a thin metal film as a probe of its microenvironment through enhanced light scattering and fluorescence,” *J. Opt. Soc. Am. B* 3, 1239-1244 (1986).
- [15] H. Rigneault, J. Capoulade, J. Dintinger, J. Wenger, N. Bonod, E. Popov, T. W. Ebbesen, P.-F. Lenne, “Enhancement of single-molecule fluorescence detection in subwavelength apertures,” *Phys. Rev. Lett.* 95, 117401 (2005).
- [16] D. Gérard, J. Wenger, N. Bonod, E. Popov, H. Rigneault, F. Mahdavi, S. Blair, J. Dintinger, and T. W. Ebbesen, “Nanoaperture-enhanced fluorescence: Towards higher detection rates with plasmonic metals,” *Phys. Rev. B* 77, 045413 (2008).
- [17] E. Popov, M. Nevière, J. Wenger, P.-F. Lenne, H. Rigneault, P. Chaumet, N. Bonod, J. Dintinger, T.W. Ebbesen, “Field enhancement in single subwavelength apertures,” *J. Opt. Soc. Am. A* 23, 2342-2348 (2006).
- [18] Mahdavi, F., Blair, S. “Nanoaperture fluorescence enhancement in the ultraviolet,” *Plasmonics* 5, 162-169 (2010).

- [19] Aouani, H.; Wenger, J.; Gérard, D.; Rigneault, H.; Devaux, E.; Ebbesen, T. W.; Mahdavi, F.; Xu, T.; Blair, S. "Crucial Role of the Adhesion Layer on the Plasmonic Fluorescence Enhancement," *ACS Nano* 3, 2043-2048 (2009).
- [20] Wenger, J.; Aouani, H.; Gérard, D.; Blair, S.; Ebbesen, T. W.; Rigneault, H. "Enhanced fluorescence from metal nanoapertures: physical characterizations and biophotonic applications," *Proc. of SPIE* 7577, 75770J (2010).
- [21] Wenger, J.; Gérard, D.; Bonod, N.; Popov, E.; Rigneault, H.; Dintinger, J.; Mahboub, O.; Ebbesen, T. W. "Emission and excitation contributions to enhanced single molecule fluorescence by gold nanometric apertures," *Opt. Express* 16, 3008-3020 (2008).
- [22] Mahdavi F, Liu Y, Blair S, "Modeling Fluorescence Enhancement from Metallic Nanocavities," *Plasmonics* 2, 129-142 (2007).
- [23] Aouani, H.; Itzhakov, S.; Gachet, D.; Devaux, E.; Ebbesen, T. W.; Rigneault, H.; Oron, D.; Wenger, J. "Colloidal Quantum Dots as Probes of Excitation Field Enhancement in Photonic Antennas," *ACS Nano* 4, 4571-4578 (2010).
- [24] T.-D. Onuta, M. Waegle, C. C. DuFort, W. L. Schaich, B. Dragnea, "Optical Field Enhancement at Cusps between Adjacent Nanoapertures," *Nano Lett.* 7, 557-564 (2007).
- [25] P. Schön, N. Bonod, E. Devaux, J. Wenger, H. Rigneault, T.W. Ebbesen, and S. Brasselet, "Enhanced second-harmonic generation from individual metallic nanoapertures," *Opt. Lett.* 35, 4063-4065 (2010).
- [26] N. Djaker, R. Hostein, E. Devaux, T. W. Ebbesen, H. Rigneault, J. Wenger, "Surface Enhanced Raman Scattering on a Single Nanometric Aperture," *J. Phys. Chem. C* 114, 16250-16256 (2010).
- [27] E. Verhagen, L. Kuipers, A. Polman, "Field enhancement in metallic subwavelength aperture arrays probed by erbium upconversion luminescence," *Opt. Express* 17, 14586-14598 (2009).
- [28] J. S. White, G. Veronis, Z. Yu, E. S. Barnard, A. Chandran, S. Fan, M. L. Brongersma, "Extraordinary optical absorption through subwavelength slits," *Opt. Lett.* 34, 686-688 (2009).
- [29] Y. C. Jun, R. Pala, M. L. Brongersma, "Strong Modification of Quantum Dot Spontaneous Emission via Gap Plasmon Coupling in Metal Nanoslits," *J. Phys. Chem. C* 114, 7269-7273 (2010).
- [30] J. Wenger, P.-F. Lenne, E. Popov, H. Rigneault, J. Dintinger, T.W. Ebbesen, "Single molecule fluorescence in rectangular nano-apertures," *Opt. Express* 13, 7035-7044 (2005).
- [31] G. Colas des Francs, D. Molenda, U. C. Fischer, A. Naber, "Enhanced light confinement in a triangular aperture: Experimental evidence and numerical calculations," *Phys. Rev. B* 72, 165111 (2005).
- [32] F. I. Baida, A. Belkhir, D. Van Labeke, "Subwavelength metallic coaxial waveguides in the optical range: Role of the plasmonic modes," *Phys. Rev. B* 74, 205419 (2006).

- [33] E. J. R. Vesseur, F. J. Garcia de Abajo, A. Polman, “Broadband Purcell enhancement in plasmonic ring cavities,” *Phys. Rev. B* 82, 165419 (2010).
- [34] A. Degiron, H. J. Lezec, N. Yamamoto, T. W. Ebbesen, “Optical transmission properties of a single subwavelength aperture in a real metal,” *Opt. Commun.* 239, 61-66 (2004).
- [35] Gersen, H.; Garcia-Parajo, M. F.; Novotny, L.; Veerman, J. A.; Kuipers, L.; van Hulst, N. F., “Influencing the Angular Emission of a Single Molecule,” *Phys. Rev. Lett.* 85, 5312-5315 (2000).
- [36] H. J. Lezec, A. Degiron, E. Devaux, et al., “Beaming light from a subwavelength aperture,” *Science* 297, 820-822 (2002).
- [37] A. Nahata, R. A. Linke, T. Ishi and K. Ohashi, “Enhanced nonlinear optical conversion from a periodically nanostructured metal film,” *Opt. Lett.* 28, 423-425 (2003).
- [38] H. Aouani, O. Mahboub, N. Bonod, E. Devaux, E. Popov, H. Rigneault, T.W. Ebbesen, J. Wenger, “Bright unidirectional fluorescence emission of molecules in a nanoaperture with plasmonic corrugations,” *Nano Lett.* 11, 637-644 (2011).
- [39] H. Aouani, O. Mahboub, E. Devaux, H. Rigneault, T.W. Ebbesen, J. Wenger, “Plasmonic Antennas for Directional Sorting of Fluorescence Emission,” *Nano Lett.* 11, 2400-2406 (2011).
- [40] Jun, Y. C.; Huang, K. C. Y.; Brongersma, M. L., “Plasmonic beaming and active control over fluorescent emission,” *Nature Commun.* 2, 283 (2011).
- [41] Martin-Moreno, L.; Garcia-Vidal, F. J.; Lezec, H. J.; Degiron, A.; Ebbesen, T. W., “Theory of Highly Directional Emission from a Single Subwavelength Aperture Surrounded by Surface Corrugations,” *Phys. Rev. Lett.* 90, 167401 (2003).
- [42] Carretero-Palacios, S.; Mahboub, O.; Garcia-Vidal, F. J.; Martin-Moreno, L.; Rodrigo, S. G.; Genet, C.; Ebbesen, T. W. “Mechanisms for Extraordinary Optical Transmission through bull’s eye structures,” *Opt. Express*, 19, 10429-10442 (2011).
- [43] Mahboub, O.; Carretero-Palacios, S.; Genet, C.; Garcia-Vidal, F. J.; Rodrigo, S. G.; Martin-Moreno, L.; Ebbesen, T. W. “Optimization of bulls eye structures for transmission enhancement,” *Opt. Express* 18, 11292-11299 (2010).
- [44] H. Aouani, O. Mahboub, E. Devaux, H. Rigneault, T.W. Ebbesen, J. Wenger, “Large molecular fluorescence enhancement by a nanoaperture with plasmonic corrugations,” *Opt. Express* 19, 13056-13062 (2011).
- [45] N. Bonod, E. Popov, D. Gérard, J. Wenger, and H. Rigneault, “Field enhancement in a circular aperture surrounded by a single channel groove,” *Opt. Express* 16, 2276-2287 (2008).
- [46] Q. Min, M. J. Leite Santos, E. M. Girotto, A. G. Brolo, R. Gordon, “Localized Raman Enhancement from a Double-Hole Nanostructure in a Metal Film,” *J. Phys. Chem. C* 112, 15098-15101 (2008).

- [47] Genevet, P.; Tetienne, J.-P.; Gatzogiannis, E.; Blanchard, R.; Kats, M. A.; Scully, M. O.; Capasso, F., "Large Enhancement of Nonlinear Optical Phenomena by Plasmonic Nanocavity Gratings," *Nano Lett.* 10, 4880-4883 (2010).
- [48] Wang, D.; Yang, T.; Crozier, K. B., "Optical antennas integrated with concentric ring gratings: electric field enhancement and directional radiation," *Opt. Express* 19, 2148-2157 (2011).
- [49] B. Liu, D. Wang, C. Shi, K. B. Crozier, T. Yang, "Vertical optical antennas integrated with spiral ring gratings for large local electric field enhancement and directional radiation," *Opt. Express* 19, 10049-10056 (2011).
- [50] Y. Liu and S. Blair, "Fluorescence enhancement from an array of subwavelength metal apertures," *Opt. Lett.* 28, 507-509 (2003).
- [51] Y. Liu and S. Blair, "Fluorescence transmission through 1-D and 2-D periodic metal films," *Opt. Express* 12, 3686-3693 (2004).
- [52] Y. Liu, F. Mahdavi, and S. Blair, "Enhanced fluorescence transduction properties of metallic nanocavity arrays," *IEEE J. Sel. Top. Quantum Electron.* 11, 778-784 (2005).
- [53] A. G. Brolo, S. C. Kwok, M. G. Moffitt, R. Gordon, J. Riordon, and K. L. Kavanagh, "Enhanced fluorescence from arrays of nanoholes in a gold film," *J. Am. Chem. Soc.* 127, 14936-14941 (2005).
- [54] A. G. Brolo, S. C. Kwok, M. D. Cooper, M. G. Moffitt, C.-W. Wang, R. Gordon, J. Riordon, and K. L. Kavanagh, "Surface Plasmon-Quantum Dot Coupling from Arrays of Nanoholes," *J. Phys. Chem. B* 110, 8307-8313 (2006).
- [55] J. H. Kim and P. J. Moyer, "Laser-induced fluorescence within subwavelength metallic arrays of nanoholes indicating minimal dependence upon hole periodicity," *Appl. Phys. Lett.* 90, 131111 (2007).
- [56] P.-F. Guo, S. Wu, Q.-J. Ren, J. Lu, Z. Chen, S.-J. Xiao, Y.-Y. Zhu, "Fluorescence Enhancement by Surface Plasmon Polaritons on Metallic Nanohole Arrays," *J. Phys. Chem. Lett.* 1, 315-318 (2010).
- [57] E. J. A. Kroekenstoel, E. Verhagen, R. J. Walters, L. Kuipers, A. Polman, "Enhanced spontaneous emission rate in annular plasmonic nanocavities," *Appl. Phys. Lett.* 95, 263106 (2009).
- [58] E. Verhagen, L. Kuipers, A. Polman, "Field enhancement in metallic subwavelength aperture arrays probed by erbium upconversion luminescence," *Opt. Express* 17, 14586-14598 (2009).
- [59] M. Airola, Y. Liu, S. Blair, "Second-harmonic generation from an array of sub-wavelength metal apertures," *J. Opt. A: Pure Appl. Opt.* 7, S118-S123 (2005).
- [60] J. A. H. van Nieuwstadt, M. Sandtke, R. H. Harmsen, F. B. Segerink, J. C. Prangsma, S. Enoch, L. Kuipers, "Strong Modification of the Nonlinear Optical Response of Metallic Subwavelength Hole Arrays," *Phys. Rev. Lett.* 97, 146102 (2006).

- [61] M.J. Levene, J. Korlach, S.W. Turner, M. Foquet, H.G. Craighead, W.W. Webb, "Zero-mode waveguides for single-molecule analysis at high concentrations," *Science* 299, 682-686 (2003).
- [62] K. T. Samiee, M. Foquet, L. Guo, E. C. Cox, H. G. Craighead, "Lambda repressor oligomerization kinetics at high concentrations using fluorescence correlation spectroscopy in zero-mode waveguides," *Biophys. J.* 88, 2145-2153 (2005).
- [63] J. T. Mannion, and H. G. Craighead, "Nanofluidic structures for single biomolecule fluorescent detection," *Biopolymers* 85, 131-143 (2007).
- [64] J. Wenger, H. Rigneault, "Photonic Methods to Enhance Fluorescence Correlation Spectroscopy and Single Molecule Fluorescence Detection," *Int. J. Mol. Sci.* 11, 206-221 (2010).
- [65] J. Wenger, D. Grard, P.-F. Lenne, H. Rigneault, J. Dintinger, T.W. Ebbesen, A. Boned, F. Conchonaud, D. Marguet, "Dual-color fluorescence cross-correlation spectroscopy in a single nanoaperture : towards rapid multicomponent screening at high concentrations," *Opt. Express* 14, 12206-12216 (2006).
- [66] J. Wenger, D. Gérard, H. Aouani, B. Lowder, S. Blair, E. Devaux, and T.W. Ebbesen, "Nanoaperture-Enhanced Signal-to-Noise Ratio in Fluorescence Correlation Spectroscopy," *Anal. Chem.* 81, 834-839 (2009).
- [67] T. Miyake, T. Tanii, H. Sonobe, R. Akahori, N. Shimamoto, T. Ueno, T. Funatsu, I. Ohdomari, "Real-Time Imaging of Single-Molecule Fluorescence with a Zero-Mode Waveguide for the Analysis of Protein-Protein Interaction," *Anal. Chem.* 80, 6018-6022 (2008).
- [68] Eid, J.; Fehr, A.; Gray, J.; Luong, K.; et al. "Real-Time DNA Sequencing from Single Polymerase Molecules," *Science* 323, 133-138 (2009).
- [69] McNally, B. ; Singer, A.; Yu, Z. ; Sun, Y. ; Weng, Z. ; Meller, A. "Optical Recognition of Converted DNA Nucleotides for Single-Molecule DNA Sequencing Using Nanopore Arrays," *Nano Lett.* 10, 2237-2244 (2010).
- [70] Korlach J, Marks PJ, Cicero RL, Gray JJ, Murphy DL, Roitman DB, Pham TT, Otto GA, Foquet M, Turner SW, "Selective aluminum passivation for targeted immobilization of single DNA polymerase molecules in zero-mode waveguide nanostructures," *Proc. Natl. Acad. Sci. USA* 105, 1176-1181 (2008).
- [71] D. Marguet, P.-F. Lenne, H. Rigneault, and H.-T. He, "Dynamics in the plasma membrane: how to combine fluidity and order," *EMBO J.* 25, 3446-3457 (2006).
- [72] J. B. Edel, M. Wu, B. Baird, H. G. Craighead, "High spatial resolution observation of single molecule dynamics in living cell membranes," *Biophys. J.* 88, L43-L45 (2005).
- [73] K. T. Samiee, J. M. Moran-Mirabal, Y. K. Cheung, H. G. Craighead, "Zero Mode Waveguides for Single-Molecule Spectroscopy on Lipid Membranes," *Biophys. J.* 90, 3288-3299 (2006).

- [74] J. Wenger, F. Conchonaud, J. Dintinger, L. Wawrezinieck, T. W. Ebbesen, H. Rigneault, D. Marguet, P. F. Lenne, "Diffusion Analysis within Single Nanometric Apertures Reveals the Ultrafine Cell Membrane Organization," *Biophys. J.* 92, 913-919 (2007).
- [75] L. Wawrezinieck, H. Rigneault, D. Marguet, and P. F. Lenne, "Fluorescence correlation spectroscopy diffusion laws to probe the submicron cell membrane organization," *Biophys. J.* 89, 4029-4042 (2005).
- [76] J. Wenger, H. Rigneault, J. Dintinger, D. Marguet, P. F. Lenne, "Single-fluorophore diffusion in a lipid membrane over a subwavelength aperture," *J. Biol. Phys.* 32, SN1-SN4 (2006).
- [77] J. M. Moran-Mirabal, A. J. Torres, K. T. Samiee, B. Baird, and H. G. Craighead, "Cell investigation of nanostructures: zero-mode waveguides for plasma membrane studies with single molecule resolution," *Nanotechnology* 18, 195101 (2007).
- [78] C. V. Kelly, B. A. Baird, H. G. Craighead, "An Array of Planar Apertures for Near-Field Fluorescence Correlation Spectroscopy," *Biophys. J.* 100, L34-L36 (2011).
- [79] M. L. Juan, M. Righini, R. Quidant, "Plasmon nano-optical tweezers," *Nature Photon.* 5, 349-356 (2011).
- [80] M. L. Juan, R. Gordon, Y. Pang, F. Eftekhari, R. Quidant, "Self-induced back-action optical trapping of dielectric nanoparticles," *Nature Phys.* 5, 915-919 (2009).
- [81] Krishnan, A., T. Thio, T. J. Kim, H. J. Lezec, T. W. Ebbesen, P. A. Wolff, J. Pendry, L. Martin-Moreno, and F. J. Garcia-Vidal, "Evanescently coupled resonance in surface plasmon enhanced transmission," *Opt. Commun.* 200, 1-7 (2001).
- [82] A. G. Brolo, R. Gordon, B. Leathem, and K. L. Kavanagh, "Surface Plasmon Sensor Based on the Enhanced Light Transmission through Arrays of Nanoholes in Gold Films," *Langmuir* 20, 4813-4815 (2004).
- [83] P. R. H. Stark, A. E. Halleck, D. N. Larson, "Short order nanohole arrays in metals for highly sensitive probing of local indices of refraction as the basis for a highly multiplexed biosensor technology," *Methods* 37, 37-47 (2005).
- [84] K. A. Tetz, L. Pang, Y. Fainman, "High-resolution surface plasmon resonance sensor based on linewidth-optimized nanohole array transmittance," *Opt. Lett.* 31, 1528-1530 (2006).
- [85] A. De Leebeeck, L. K. S. Kumar, V. de Lange, D. Sinton, R. Gordon, and A. G. Brolo, "On-Chip Surface-Based Detection with Nanohole Arrays," *Anal. Chem.* 79, 4094-4100 (2007).
- [86] J. C. Sharpe, J. S. Mitchell, L. Lin, N. Sedoglavich, R. J. Blaikie, "Gold Nanohole Array Substrates as Immunobiosensors," *Anal. Chem.* 80, 2244-2249 (2008).
- [87] A. Lesuffleur, H. Im, N. C. Lindquist, K. S. Lim, S.-H. Oh, "Laser-illuminated nanohole arrays for multiplex plasmonic microarray sensing," *Opt Express* 16, 219-224 (2008).

- [88] A. Lesuffleur, H. Im, N. C. Lindquist, S.-H. Oh, "Periodic nanohole arrays with shape-enhanced plasmon resonance as real-time biosensors," *Appl. Phys. Lett.* 90, 243110 (2007).
- [89] H. Im, A. Lesuffleur, N. C. Lindquist, S.-H. Oh, "Plasmonic Nanoholes in a Multichannel Microarray Format for Parallel Kinetic Assays and Differential Sensing," *Anal. Chem.* 81, 2854-2859 (2009).
- [90] J.-C. Yang, J. Ji, J. M. Hogle, D. N. Larson, "Metallic Nanohole Arrays on Fluoropolymer Substrates as Small Label-Free Real-Time Bioprobes," *Nano Lett.* 8, 2718-2724 (2008).
- [91] J. Ji, J. G. OConnell, D. J. D. Carter, D. N. Larson, "High-Throughput Nanohole Array Based System To Monitor Multiple Binding Events in Real Time," *Anal. Chem.* 80, 2491-2498 (2008).
- [92] J. Prikulis, P. Hanarp, L. Olofsson, D. Sutherland, and M. Käll, "Optical Spectroscopy of Nanometric Holes in Thin Gold Films," *Nano Lett.* 4, 1003-1007 (2004).
- [93] Rindzevicius, T., Y. Alaverdyan, A. Dahlin, F. Hook, D. S. Sutherland, M. Kall, "Plasmonic Sensing Characteristics of Single Nanometric Holes," *Nano Lett.* 5, 2335-2339 (2005).
- [94] A. Dahlin, M. Zäch, T. Rindzevicius, M. Käll, D. S. Sutherland, and F. Höök, "Localized Surface Plasmon Resonance Sensing of Lipid-Membrane-Mediated Biorecognition Events," *J. Am. Chem. Soc.* 127, 5043-5048 (2005).
- [95] M. P. Jonsson, P. Jönsson, A. B. Dahlin, F. Höök, "Supported Lipid Bilayer Formation and Lipid-Membrane-Mediated Biorecognition Reactions Studied with a New Nanoplasmonic Sensor Template," *Nano Lett.* 7, 3462-3468 (2007).
- [96] D. Gao, W. Chen, A. Mulchandani, and J. S. Schultz, "Detection of tumor markers based on extinction spectra of visible light passing through gold nanoholes," *Appl. Phys. Lett.* 90, 073901 (2007).
- [97] M. P. Jonsson, A. B. Dahlin, L. Feuz, S. Petronis, F. Höök, "Locally Functionalized Short-Range Ordered Nanoplasmonic Pores for Bioanalytical Sensing," *Anal. Chem.* 82, 2087-2094 (2010).
- [98] S. M. Williams, A. D. Stafford, K. R. Rodriguez, T. M. Rogers, J. V. Coe, "Accessing Surface Plasmons with Ni Microarrays for Enhanced IR Absorption by Monolayers," *J. Phys. Chem. B* 107, 11871-11879 (2003).
- [99] S. M. Williams, et al., "Use of the extraordinary infrared transmission of metallic subwavelength arrays to study the catalyzed reaction of methanol to formaldehyde on copper oxide," *J. Phys. Chem. B* 108, 11833-11837 (2004).
- [100] S. M. Teeters-Kennedy, et al., "Controlling the Passage of Light through Metal Microchannels by Nanocoatings of Phospholipids," *J. Phys. Chem. B* 110, 21719-21727 (2006).
- [101] J. Dintinger, S. Klein, and T. W. Ebbesen, "MoleculeSurface Plasmon Interactions in Hole Arrays: Enhanced Absorption, Refractive Index Changes, and All-Optical Switching," *Adv. Mater.* 18, 1267-1270 (2006).

- [102] J. Dintinger, I. Robel, P. V. Kamat, C. Genet, and T. W. Ebbesen, "Terahertz All-Optical Molecule-Plasmon Modulation," *Adv. Mater.* 18, 1645-1648 (2006).
- [103] A. Salomon, C. Genet, T. W. Ebbesen, "MoleculeLight Complex: Dynamics of Hybrid MoleculeSurface Plasmon States," *Angew. Chem. Int. Ed.* 48, 8748-8751 (2009).
- [104] Y. Liu, J. Bishop, L. Williams, S. Blair, and J. Herron, "Biosensing based upon molecular confinement in metallic nanocavity arrays," *Nanotechnology* 15, 1368-1374 (2004).
- [105] S. Attavar, M. Diwekar, S. Blair, "Photoactivated capture molecule immobilization in plasmonic nanoapertures in the ultraviolet," *Lab Chip* 11, 841-844 (2011).
- [106] H. Ko, S. Singamaneni, V. V. Tsukruk, "Nanostructured Surfaces and Assemblies as SERS Media," *Small* 4, 1576-1599 (2008).
- [107] A. G. Brolo, E. Arctander, R. Gordon, B. Leathem, K. L. Kavanagh, "Nanohole-Enhanced Raman Scattering," *Nano Lett.* 4, 2015-2018 (2004).
- [108] J. T. Bahns, F. Yan, D. Qiu, R. Wang, L. Chen, "Hole-Enhanced Raman Scattering," *Appl. Spectrosc.* 60, 989-993 (2006).
- [109] T. H. Reilly, J. D. Corbman, K. L. Rowlen, "Vapor Deposition Method for Sensitivity Studies on Engineered Surface-Enhanced Raman Scattering-Active Substrates," *Anal. Chem.* 79, 5078-5081 (2007).
- [110] Q. Yu, G. Golden, "Probing the Protein Orientation on Charged Self-Assembled Monolayers on Gold Nanohole Arrays by SERS," *Langmuir* 23, 8659-8662 (2007).
- [111] Q. Yu, P. Guan, D. Qin, G. Golden, P. M. Wallace, "Inverted Size-Dependence of Surface-Enhanced Raman Scattering on Gold Nanohole and Nanodisk Arrays," *Nano Lett.* 8, 1923-1928 (2008).
- [112] J. R. Anema, A. G. Brolo, P. Marthandam, and R. Gordon, "Enhanced Raman Scattering from Nanoholes in a Copper Film," *J. Phys. Chem. C* 112, 17051-17055 (2008).
- [113] T. H. Reilly, S.-H. Chang, J. D. Corbman, G. C. Schatz, K. L. Rowlen, "Quantitative Evaluation of Plasmon Enhanced Raman Scattering from Nanoaperture Arrays," *J. Phys. Chem. C* 111, 1689-1694 (2007).
- [114] A. Lesuffleur, L. K. S. Kumar, A. G. Brolo, K. L. Kavanagh, R. Gordon, "Apex-Enhanced Raman Spectroscopy Using Double-Hole Arrays in a Gold Film," *J. Phys. Chem. C* 111, 2347-2350 (2007) .
- [115] H. Wei, U. Håkanson, Z. Yang, F. Höök, H. Xu, "Individual Nanometer Hole-Particle Pairs for Surface-Enhanced Raman Scattering," *Small* 4, 1296-1300 (2008).
- [116] J. T. Bahns, Q. Guo, J. M. Montgomery, S. K. Gray, H. M. Jaeger, L. Chen, "High-Fidelity Nano-Hole-Enhanced Raman Spectroscopy," *J. Phys. Chem. C* 113, 11190-11197 (2009) .

- [117] A. Drezet, C. Genet, T. W. Ebbesen, “Miniature Plasmonic Wave Plates,” *Phys. Rev. Lett.* 101, 043902 (2008).
- [118] T. Ishi, J. Fujikata, K. Makita, T. Baba and K. Ohashi, “Si Nano-Photodiode with a Surface Plasmon Antenna,” *Jpn. J. Appl. Phys.* 44, L364-L366 (2005).
- [119] Ren, F. F.; Ang, K. W.; Ye, J.; Yu, M.; Lo, G. Q.; Kwong, D. L., “Split Bulls Eye Shaped Aluminum Antenna for Plasmon-Enhanced Nanometer Scale Germanium Photodetector,” *Nano Lett.* 11, 1289-1293 (2011).
- [120] E. Laux, C. Genet, T. Skauli, T. W. Ebbesen, “Plasmonic photon sorters for spectral and polarimetric imaging,” *Nat. Photonics* 2, 161-164 (2008).
- [121] B. Guo, G. Song, L. Chen, “Plasmonic very-small-aperture lasers,” *Appl. Phys. Lett.* 91, 021103 (2007).
- [122] Yu, N.; Fan, J.; Wang, Q. J.; Plügl, C.; Diehl, L.; Edamura, T.; Yamanishi, M.; Kan, H.; Capasso, F., “Small-divergence semiconductor lasers by plasmonic collimation,” *Nature Photon.* 2, 564-570 (2008).
- [123] Yu, N., R. Blanchard, J. Fan, F. Capasso, T. Edamura, M. Yamanishi, H. Kan, “Small divergence edge-emitting semiconductor lasers with two-dimensional plasmonic collimators,” *Appl. Phys. Lett.* 93, 181101 (2008).
- [124] C. Liu, V. Kamaev, Z. V. Vardeny, “Efficiency enhancement of an organic light-emitting diode with a cathode forming two-dimensional periodic hole array,” *Appl. Phys. Lett.* 86, 143501 (2005).
- [125] W. Srituravanich, L. Pan, Y. Wang, C. Sun, D. B. Bogy, X. Zhang, “Flying plasmonic lens in the near field for high-speed nanolithography,” *Nature Mater.* 3, 733-737 (2008).
- [126] Y. Kim, S. Kim, H. Jung, E. Lee, J. W. Hahn, “Plasmonic nano lithography with a high scan speed contact probe,” *Opt. Express* 17, 19476-19485 (2009).
- [127] S. Park, J. W. Hahn, “Plasmonic data storage medium with metallic nano-aperture array embedded in dielectric material,” *Opt. Express* 17, 20203-20210 (2009).
- [128] P. Muhlschlegel, H. J. Eisler, O. J. F. Martin, B. Hecht, and D. W. Pohl, “Resonant Optical Antennas,” *Science* 308, 1607-1609 (2005).
- [129] A. Kinkhabwala, Z. F. Yu, S. H. Fan, Y. Avlasevich, K. Mullen, W. E. Moerner, “Large Single-Molecule Fluorescence Enhancements Produced by a Bowtie Nanoantenna,” *Nat. Photonics* 3, 654-657 (2009).
- [130] Punj, D., Mivelle, M., Moparthi, S.B., van Zanten, T.S., Rigneault, H., van Hulst, N.F., Garcia-Parajo, M.F., Wenger, J. A plasmonic ‘antenna-in-box’ platform for enhanced single-molecule analysis at micromolar concentrations. *Nat. Nanotechnol.* 8, 512-516 (2013).